BIOCHEMISTRY
including biophysical chemistry & molecular biology

ARTICLE

pubs.acs.org/biochemistry

Biochemical Characterization of a Multidomain Deubiquitinating Enzyme Ubp15 and the Regulatory Role of Its Terminal Domains

William P. Bozza and Zhihao Zhuang*

Department of Chemistry and Biochemistry, University of Delaware, 214A Drake Hall, Newark, Delaware 19716, United States

Supporting Information

ABSTRACT: Deubiquitinating enzymes (DUBs) have emerged as essential players in a myriad of cellular processes, yet the regulation of DUB function remains largely unknown. While some DUBs rely on the formation of complex for regulation of enzymatic activity, many DUBs utilize interdomain interactions to regulate catalysis. Here we report the biochemical characterization of a multidomain deubiquitinating enzyme, Ubp15, from *Saccharomyces cerevisiae*. Steady-state kinetic investigation showed that Ubp15 is a highly active DUB. We identified active-site residues that are required for catalysis. We have also identified key residues on Ubp15 required for ubiquitin binding and catalysis. We further demonstrated that Ubp15's enzymatic activity is regulated by the N- and C-terminal domains that flank the catalytic core domain. Moreover, we demonstrated that Ubp15 physically interacts with a WD40 repeat-containing protein, Cdh1, by copurification experiments. Interestingly, unlike other DUBs that specifically interact with WD40 repeat-containing proteins, Cdh1 does not function in stimulating Ubp15's activity. The possible cellular function of Ubp15 in cell cycle regulation is discussed in view of the specific interaction between Ubp15 and Cdh1, an activator of the anaphase-promoting complex/cyclosome (APC/C).

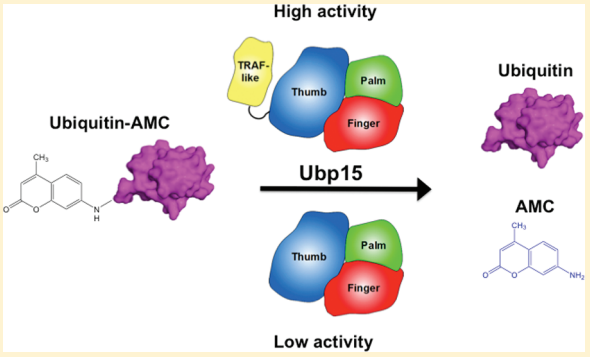

Ubiquitination has been established as an essential posttranslational modification required for numerous cellular processes, including DNA repair, cell cycle regulation, transcription, and proteasome-mediated protein degradation.[1,2] While ubiquitination has been subjected to intensive investigation, the opposing process catalyzed by the deubiquitinating enzyme (DUB) remains less well understood. There are approximately 100 DUBs in humans and 20 in yeast.[3−5] DUBs can be grouped into at least five families, including ubiquitin-specific protease (USP), ubiquitin C-terminal hydrolase (UCH), the ovarian tumor (OTU) domain DUB, the Machado-Joseph (MJD) domain DUB, and the Jab1/MPN metalloenzyme (JAMM) domain DUB.[6,7] The ubiquitin-specific proteases or the ubiquitin-specific processing proteases (Ubp) constitute the largest of the five DUB families. Many known USPs are large, multidomain proteins. The USP catalytic core is usually flanked by terminal domains on either end or both ends. While the catalytic core domain is highly conserved across the USP family, the terminal domains are significantly divergent in sequence. So far, most studies of USPs have focused on the isolated USP catalytic core. While these studies have provided an important foundation for understanding USP catalysis, investigation of the USP catalytic core in the presence of the flanking sequences is essential for a better understanding of both USP catalysis and regulation.

In recent years, the regulatory mechanism of USP function has received increasing attention. Several studies have demonstrated that DUB can be regulated by interacting protein factors. For example, the interaction of USP14 with the human proteasome was found to significantly stimulate its enzymatic activity. Only in the presence of the 19S regulatory particle (RP) of the proteasome was USP14 covalently modified by the active-site probe, ubiquitin-vinyl sulfone (UbVS).[8] The authors attributed the increase in activity to the possible movement of two surface loops that cover the enzyme active site, allowing ubiquitin's access to the USP14 active site. Activation of DUB activity by proteasome was also observed for USP14's yeast homologue, Ubp6.[9] Ubp8, likewise, requires several protein subunits in the SAGA (Spt-Ada-Gcn5-acetyltransferase) complex to be active in catalysis. Two recent structures of Ubp8 bound to Sgf11, Sus1, and Sgf73 provided important insights into how Ubp8 is activated through direct interactions between the active-site loops and ubiquitin-binding elements of the protein partners.[10,11] Protein interaction has also been found to stimulate several endosomal DUBs. The protein STAM (signal transducing adapter molecule), a component of the multivesicular body-sorting machinery, was found to increase the catalytic activity of AMSH (associated molecule with the SH3 domain of STAM) toward K63-linked ubiquitin chains.[12] Interestingly, STAM can also activate the ubiquitin-specific protease USP8/UBPY.[13]

Received: April 8, 2011
Revised: June 8, 2011
Published: June 28, 2011

However, not all DUBs require interacting protein partners for their enzymatic activity. Many USPs are large multidomain proteins, whose activity relies on regulatory domains within the same polypeptide chain. In human USP25, a predicted coiled coil region C-terminal to the catalytic core was found to be essential for catalytic activity.[14] Two studies of the human USP7 (or HAUSP) have identified the terminal domains as essential in regulating DUB activity.[15,16]

Here we report the biochemical characterization of Ubp15, a homologue of the human USP7 in *Saccharomyces cerevisiae*. We found that the N- and C-terminal domains play important roles in regulating Ubp15 catalytic activity. We conducted detailed enzyme kinetic analyses of the full-length and truncated Ubp15 proteins. We demonstrated that the N- and C-terminal domains are required for the enzymatic activity of Ubp15. We also interrogated the role of an interdomain connecting loop in catalysis. Utilizing site-directed mutagenesis, we further interrogated the specific interaction between ubiquitin and Ubp15 and its contribution to catalysis. We found that hydrogen bonding between the USP finger subdomain and the N-terminal face of ubiquitin is crucial for Ubp15's catalytic activity. In an effort to characterize the interaction between Ubp15 and a WD40 repeat-containing protein, Cdh1, we coexpressed and purified the proteins as a complex. We found that although these two proteins interact, Cdh1 does not stimulate Ubp15's activity. We also discussed the physiological role of Ubp15 in cell cycle control and its possible functional interaction with the anaphase-promoting complex/cyclosome (APC/C).

MATERIALS AND METHODS

Molecular Cloning and Plasmid Construction. The Ubp15 and Cdh1 genes were amplified from *S. cerevisiae* genomic DNA by polymerase chain reaction. To generate full-length N-terminally His-tagged Ubp15 and Cdh1, the genes were cloned into the baculovirus expression vector, pFastBac HTa (Invitrogen). The genes were cloned into the multiple-cloning site using the restriction enzymes NcoI and XhoI. To generate GST-tagged Ubp15, we replaced the His tag in the pFastBac HTa vector with a GST tag, which was subcloned from the pGEX 4T-3 vector (GE Healthcare). Subsequently, the full-length Ubp15 gene was cloned into the multiple-cloning site downstream of the newly inserted GST tag using the restriction enzymes NcoI and XhoI. Genes encoding truncated Ubp15, Ubp15(1−585), Ubp15-(196−1230), and Ubp15(196−585), were also cloned into the pFastBac vector downstream of the GST tag. We also cloned several truncated Ubp15 genes, Ubp15(1−208), Ubp15(1−585), Ubp15(188−585), Ubp15(196−585), and Ubp15(209−585), into *Escherichia coli* expression vector pET-28a using the restriction enzymes NdeI and XhoI.

Protein Expression and Purification. Full-length N-terminal His-tagged Ubp15, N-terminal His-tagged Ubp15 (196-1230), and full-length N-terminal His-tagged Cdh1 were expressed in Sf9 cells using the pFastBac HTa baculovirus expression vector. Recombinant virus was generated through bacmid transfection into Sf9 cells. After three successive passages, the virus was used to infect fresh Sf9 cells. Seventy-two hours after being infected, the cells were harvested and washed with PBS buffer [10 mM Na_2HPO_4 (pH 7.5), 1.8 mM KH_2PO_4 140 mM NaCl and 2.7 mM KCl]. The cells were resuspended in lysis buffer [50 mM NaH_2PO_4 (pH 8.0), 500 mM NaCl, 5% glycerol, 5 mM β-mercaptoethanol, and 10 mM imidazole] and lysed by sonication. The lysate was centrifuged, and the soluble fraction was bound to Ni-NTA resin (Invitrogen) and washed extensively with lysis buffer. The bound protein was eluted stepwise with lysis buffer containing 40 and 100 mM imidazole. Protein purity was analyzed using sodium dodecyl sulfate−polyacrylamide gel electrophoresis (SDS−PAGE) and Coomassie Blue staining. Pure fractions were combined and exchanged into storage buffer [50 mM Tris (pH 8.0), 150 mM NaCl, 5% glycerol, and 5 mM DTT].

The His-tagged Ubp15 truncates, Ubp15(1−208), Ubp15-(1−585), Ubp15(188−585), Ubp15(196−585), and Ubp15-(209−585), were expressed in the *E. coli* Rosetta (DE3) cell line (Novagen). The cells were cultured at 17 °C for 18 h postinduction. The *E. coli* cells were harvested and sonicated in lysis buffer [50 mM Tris (pH 8.0), 150 mM NaCl, 5% glycerol, 5 mM β-mercaptoethanol, and 10 mM imidazole]. The cell free extract was bound to Ni-NTA resin (Invitrogen) or Talon cobalt affinity resin (Clontech) and washed extensively with lysis buffer. Proteins were then eluted stepwise with lysis buffer containing 25 and 80 mM imidazole. Protein purity was assessed by SDS−PAGE and Coomassie Blue staining. Pure fractions were pooled and dialyzed into a buffer containing 50 mM Tris (pH 8.0), 50 mM NaCl, 5% glycerol, and 5 mM DTT. The dialyzed sample was then loaded onto a HiTrap Q FF anion exchange column (GE) at a flow rate of 2.0 mL/min. Bound Ubp15 was eluted using a NaCl gradient from 200 to 300 mM. Pure fractions were combined and exchanged into storage buffer [50 mM Tris (pH 8.0), 150 mM NaCl, 5% glycerol, and 5 mM DTT]. The Ubp15 active-site mutants (C214A, C214S, and H465A) and the ubiquitin binding mutants (S321A, E336A, E362A, T283A, D286A, H457A, and Y466A) were expressed and purified in a manner identical to that of the wild-type protein.

Gel Filtration Chromatography. Ubp15(1−585) and Ubp15-(196−585) were analyzed using a Superose 6 gel filtration column (GE Healthcare) connected to an ÄKTA chromatography system (GE Healthcare). The column with a 24 mL bed volume was calibrated using a 12−200 kDa molecular mass calibration kit from Sigma-Aldrich. The column was equilibrated in a buffer containing 50 mM Tris (pH 8.0), 100 mM NaCl, 2.5% glycerol, and 1 mM DTT at a flow rate of 0.5 mL/min. For a typical run, 300 μL of Ubp15 protein sample at 4.5 mg/mL was injected. Protein fractions were monitored on the basis of UV−vis absorption at 280 nm. The eluted protein fractions were further analyzed via SDS−PAGE and Coomassie Blue staining. To calculate the molecular weight of the target protein, a calibration curve was generated by plotting log M_r values of the protein standards versus the partition coefficient k_{av}. $k_{av} = (V_e - V_o)/(V_c - V_o)$, where V_o is the column void volume, V_e is the elution volume, and V_c is geometric column volume.

In Vitro Deubiquitination Assay and Steady-State Kinetic Measurement. The in vitro deubiquitination activity of Ubp15 was assayed using ubiquitin-AMC (BioMol) as a substrate. Ub-AMC (ubiquitin-7-amino-4-methylcoumarin) was incubated in reaction buffer [50 mM HEPES (pH 7.8), 1 mM DTT, 0.5 mM EDTA, and 0.1 mg/mL BSA] at 25 °C. The fluorescence signal was measured using a Fluoromax-4 fluorescence spectrophotometer (Horiba) following the addition of enzyme. The initial rate was plotted versus substrate concentrations ranging from 25 nM to 1.5 μM. The steady-state rate constant was determined by fitting the initial rates to the Michaelis−Menten equation $V = (V_{max}[S])/([S] + K_m)$ using GraphPad Prism (GraphPad Software, La Jolla, CA). The equation $k_{cat} = V_{max}/[E]$ was used to determine the k_{cat} value.

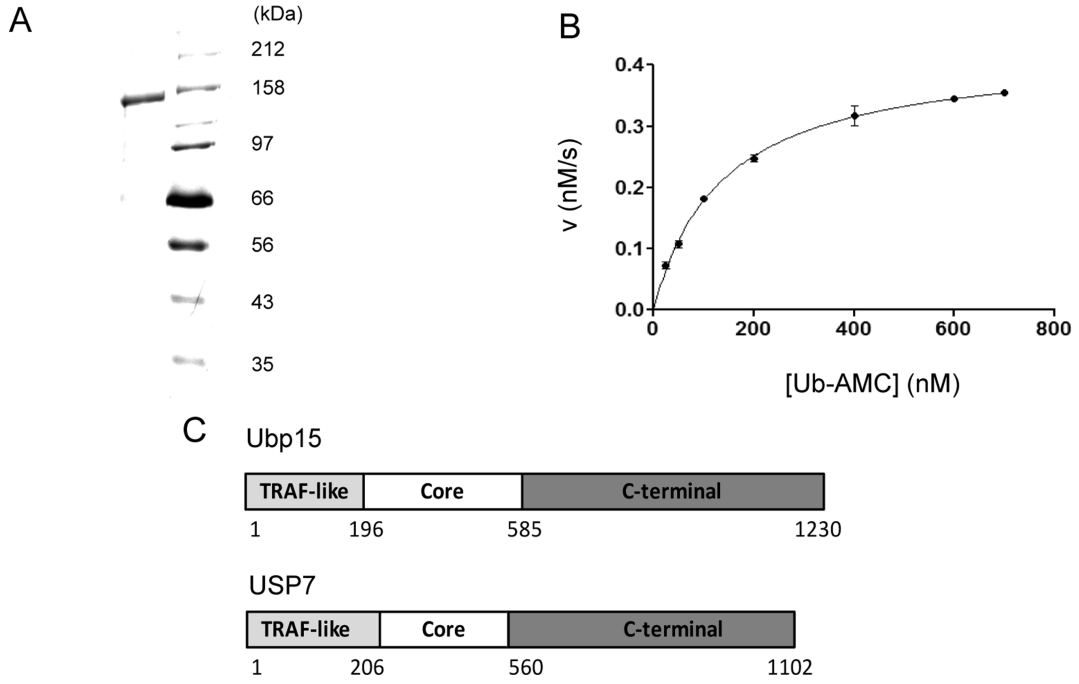

Figure 1. Ubp15 is a multidomain deubiquitinating enzyme. (A) SDS−PAGE analysis of purified full-length Ubp15. (B) Initial velocity analysis of Ubp15-catalyzed hydrolysis of Ub-AMC. The initial rate is plotted vs Ub-AMC concentration and fitted to the Michaelis−Menten equation. (C) Schematic representation of the potential domain structure of full-length Ubp15 in relation to USP7.

Circular Dichroism Spectroscopy. Circular dichroism (CD) spectra were recorded using a Jasco J-810 spectropolarimeter. CD data were collected for each sample in a 1 mm cell with 1.7 μM protein in buffer containing 10 mM $KHPO_4$ (pH 8.0), 50 mM KF, and 1 mM tris(2-carboxyethyl)phosphine. Spectra were obtained by averaging three independent data sets collected every 0.25 nm with an averaging time of 1 s and a bandwidth of 2 nm.

Guanidine Hydrochloride Denaturation. The Ubp15 core truncates (amino acids 209−585 and 196−585) at a concentration of 1.7 μM were treated with guanidine hydrochloride (0−5 M) at 25 °C for 30 min so they could reach equilibrium. CD measurements were then taken as described above. The helical content was calculated from MRE values at 222 nm using the following equation: % α-helix = $(MRE_{222} - 2340/30300) \times 100$.[17]

Purification of the Ubp15/Cdh1 Complex following Co-expression in Sf9 Cells. The recombinant viruses harboring the N-terminally His-tagged Cdh1 and the N-terminally GST-tagged Ubp15 were used to co-infect Sf9 cells; 72 h after being infected, the cells were harvested and washed with PBS buffer [10 mM Na_2HPO_4 (pH 7.5), 1.8 mM KH_2PO_4, 140 mM NaCl, and 2.7 mM KCl]. The complex was purified by affinity chromatography using either Ubp15's GST tag or Cdh1's His tag. In the former case, cells were resuspended in lysis buffer [10 mM Na_2HPO_4 (pH 7.5), 1.8 mM KH_2PO_4, 140 mM NaCl, 2.7 mM KCl, 5% glycerol, and 0.5 mM DTT] and lysed by sonication. Soluble lysate was bound to glutathione Sepharose (GE Healthcare) and washed extensively with lysis buffer. The bound complex was eluted from the resin using elution buffer [50 mM Tris (pH 7.5), 100 mM NaCl, 10% glycerol, and 20 mM reduced glutathione]. The purified protein complex was detected using SDS−PAGE and Coomassie Blue staining. To purify the complex using Cdh1's His tag, cells were resuspended and lysed in buffer containing 50 mM NaH_2PO_4 (pH 8.0), 100 mM NaCl, 5% glycerol, 5 mM β-mercaptoethanol, and 10 mM imidazole. Soluble lysate was bound to Ni-NTA (Invitrogen) and washed extensively with the same buffer. The Ubp15/Cdh1 complex was eluted with a buffer containing 100 mM imidazole. Formation of the complex was detected using SDS−PAGE and Coomassie Blue staining.

The viruses harboring GST-Ubp15(1−585), GST-Ubp15-(196−1230), or GST-Ubp15(196−585) were used to co-infect Sf9 cells with His-tagged Cdh1 in a manner identical to that used for full-length Ubp15. The complex was purified using glutathione Sepharose resin as described for the full-length protein.

Western Blot Analysis of Ubp15/Cdh1 Protein Complexes. The protein complex purified using glutathione affinity resin was separated by SDS−PAGE and transferred to a Hybond-ECL membrane (GE Healthcare). The transfer was conducted at 30 V overnight at 4 °C in a buffer containing 25 mM Tris (pH 8.3), 200 mM glycine, and 20% methanol. The following wash and incubation steps were performed at room temperature. After each incubation step, the membrane was extensively washed with TBS-T buffer [25 mM Tris (pH 7.5), 150 mM NaCl, 2.5 mM KCl, and 0.05% Tween 20]. Following transfer, the membrane was blocked in TBS-T buffer containing 3% BSA for 60 min. The membrane was then incubated with anti-His tag primary antibodies produced in mouse (GenScript) at a dilution of 1:5000 in TBS-T buffer for 90 min. The membrane was then incubated with secondary antibody (goat anti-mouse IgG-HRP, Sigma-Aldrich) diluted 1:80000 in TBS-T buffer for 60 min. Antibody binding was visualized by incubation with an enhanced chemiluminescent substrate (Thermo scientific) for detection of HRP. The chemiluminescent signal was captured using the FluorChem Q imaging system (Cell Biosciences).

RESULTS

Ubp15 Is a Bona Fide Deubiquitinating Enzyme. The full-length Ubp15 gene was cloned into the pFastBac HTa vector and

Table 1. Steady-State Kinetic Parameters of Full-Length and Truncated Ubp15

Ubp15 construct	k_{cat} (s^{-1})	K_m (μM)	k_{cat}/K_m (M^{-1} s^{-1})	x-fold decrease in k_{cat}/K_m
Ubp15 full-length	3.24 ± 0.08	0.14 ± 0.01	2.3×10^7	1
Ubp15(1−585)	0.71 ± 0.02	0.11 ± 0.01	6.5×10^6	4
Ubp15(209−585)	no activity			
Ubp15(188−585)	0.041 ± 0.001	0.16 ± 0.02	2.6×10^5	88
Ubp15(196−585)	0.045 ± 0.002	0.11 ± 0.02	4.1×10^5	56
Ubp15(196−1230)	0.94 ± 0.02	0.10 ± 0.01	9.4×10^6	2
GST-Ubp15 full-length	1.23 ± 0.02	0.12 ± 0.01	1.0×10^7	
GST-Ubp15(1−585)	0.26 ± 0.03	0.11 ± 0.01	2.4×10^6	
GST-Ubp15(196−585)	0.074 ± 0.002	0.17 ± 0.01	4.4×10^5	
GST-Ubp15(196−1230)	1.20 ± 0.03	0.17 ± 0.01	7.1×10^6	

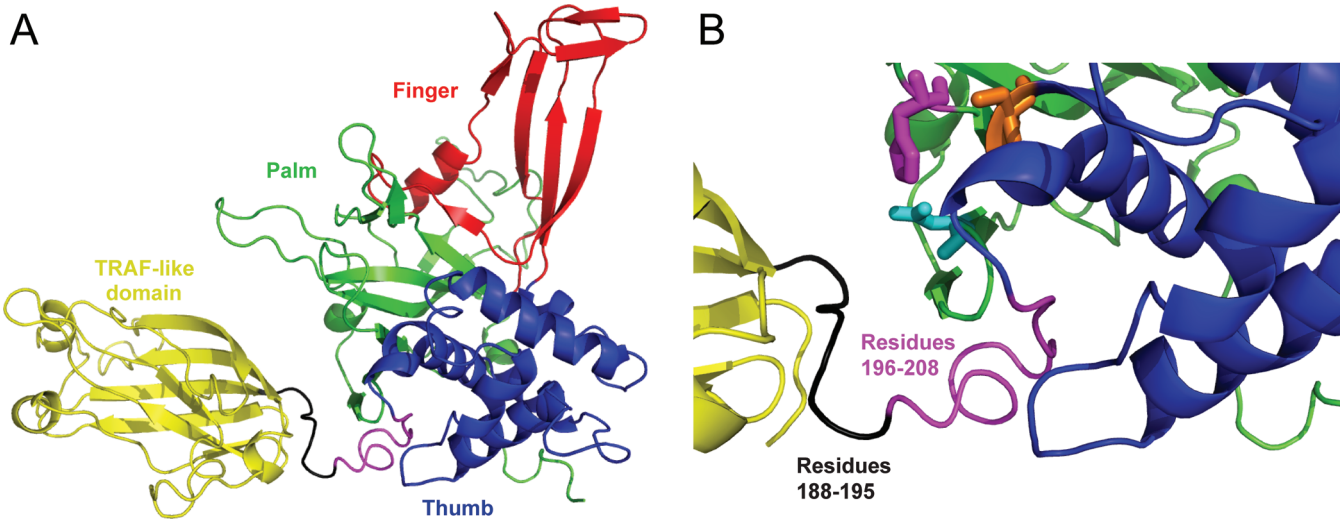

Figure 2. (A) Modeled structure of Ubp15 that contains the N-terminal TRAF-like domain and the catalytic core domain. The model was generated by the PHYRE protein fold recognition server[19] using the USP7(53−560) X-ray crystal structure as a template.[20] The N-terminal TRAF-like domain is colored yellow. The palm, thumb, and finger subdomains of the catalytic core are colored green, blue, and red, respectively. The N-terminal TRAF-like domain and the Ubp15 catalytic core are connected through a flexible loop region (residues 188−195 colored black and residues 196−208 colored magenta). (B) Close-up view of Ubp15's active site and the interdomain connecting loop. The catalytic residues C214, H465, and D482 are colored orange, magenta, and cyan, respectively. This image was generated using PyMol.

expressed in Sf9 cells. The protein was purified using nickel affinity chromatography (Figure 1A). Kinetic characterization of the full-length Ubp15 is described in Materials and Methods. Ubp15's activity of hydrolyzing Ub-AMC was monitored by fluorescence emission at 440 nm (Figure S1A of the Supporting Information). The initial velocity was plotted versus Ub-AMC concentration, and the steady-state rate constants were determined using nonlinear regression curve fitting (Figure 1B). A k_{cat} value of 3.24 ± 0.08 s^{-1} and a k_{cat}/K_m value of 2.3×10^7 M^{-1} s^{-1} were determined for full-length Ubp15 (see Table 1).

The Terminal Domains of Ubp15 Are Required for Deubiquitination Activity. We identified several putative domains in Ubp15 through sequence analysis (Figure 1C). The domain organization is similar to that of its human homologue, USP7. Ubp15's central domain (amino acids 196−585) contains the conserved Cys and His boxes that harbor the catalytic triad residues. The protease core is flanked by N- and C-terminal domains. On the basis of sequence homology, we identified a TRAF-like domain (amino acids 1−195) N-terminal to the catalytic core domain. The TNF receptor-associated factor (TRAF) domain contains seven antiparallel p-helices that functions in protein−protein interactions.[18] The TRAF-like domains are extensively represented in proteins involved in protein processing and ubiquitination. On the basis of the sequence similarity to USP7, we were able to generate a modeled structure of Ubp15 that contains the N-terminal TRAF-like domain and the catalytic core domain (Figure 2). The model was generated by the PHYRE protein fold recognition server[19] using the USP7(53−560) X-ray crystal structure as a template.[20] Fold recognition programs failed to identify homologous protein structures for the C-terminal domain.

To probe the function of the N- and C-terminal domains, we generated a truncation that contains only the Ubp15 catalytic core domain, Ubp15(196−585). Remarkably, we observed a large decrease (56-fold) in the catalytic efficiency ($k_{cat}/K_m = 4.1 \times 10^5$ M^{-1} s^{-1}) as compared to that of full-length Ubp15 (see Table 1 and Figure S1B of the Supporting Information). We also generated truncated Ubp15 proteins with either the N- or C-terminal domain removed. We found that truncation of either terminal domain reduced Ubp15's catalytic activity moderately. Removal of the N-terminal TRAF-like domain (amino acids 1−195) resulted in a 2-fold decrease in catalytic efficiency [$k_{cat}/K_m = 9.4 \times 10^6$ M^{-1}

s^{-1} (Table 1 and Figure S1B of the Supporting Information)]. Similarly, removal of the C-terminal domain (residues 586−1230) led to a 4-fold decrease in catalytic efficiency [$k_{cat}/K_m = 6.5 \times 10^6$ M^{-1} s^{-1} (Table 1 and Figure S1B of the Supporting Information)]. In both cases, the K_m was only minimally affected, suggesting that Ub-AMC binding was likely not affected by the terminal domain truncation. Together, these results suggest that the two terminal domains have a partially redundant function in stimulating the catalytic activity of the Ubp15 core domain.

We ruled out the possibility that the decrease in catalytic activity in the Ubp15 core domain is caused by protein aggregation using gel filtration chromatography. For Ubp15(196−585) and Ubp15(1−585), the protein eluted as a single peak based on UV−vis absorbance at 280 nm on a Superose 6 column (Figure S2 of the Supporting Information). The calculated molecular masses of 53 and 76 kDa for Ubp15(196−585) and Ubp15-(1−585) agree well with the predicted molecular masses of the monomeric proteins (49 and 73 kDa, respectively). The purity of the eluted protein in the peak fraction was demonstrated by SDS−PAGE and Coomassie Blue staining.

Stimulation of the Ubp15 Catalytic Core Domain by the N-Terminal TRAF-like Domain Occurs in Cis. We showed that the N-terminal TRAF-like domain stimulates the activity of the Ubp15 catalytic core domain when both domains reside in the same polypeptide. To determine whether this stimulation could also occur in trans, the purified Ubp15 N-terminal TRAF-like domain (amino acids 1−208) was incubated with the Ubp15 catalytic core domain (amino acids 196−585). The protein mixture was then added to an assay solution containing 100 nM Ub-AMC to determine the deubiquitinating activity. We found no detectable increase in activity for the Ubp15 core domain even when 10-fold more N-terminal TRAF-like domain was included (Figure S3 of the Supporting Information). We then repeated the experiment in an identical manner with the Ubp15(209−585) truncated core domain (vide infra). We found that with the addition of 10-fold more N-terminal TRAF-like domain, the Ubp15 core (amino acids 209−585) remained largely inactive. This observation suggests that the N-terminal TRAF-like domain stimulates Ubp15's activity in cis.

Assessing the Contribution of the Interdomain Loop to Ubp15's Activity. On the basis of structural modeling, we identified a loop region between the N-terminal TRAF-like domain and the catalytic core domain (Figure 2). Given that amino acids 188−208 constitute the complete linker sequence that connects the catalytic core domain to the N-terminal TRAF-like domain, we generated a Ubp15 truncate (amino acids 188−585) that contains the full linker sequence. We found that Ubp15(188−585) possesses a catalytic efficiency [$k_{cat}/K_m = 2.6 \times 10^5$ M^{-1} s^{-1} (Table 1 and Figure S1 of the Supporting Information)] similar to that of Ubp15(196−585).

We also generated a catalytic core domain (amino acids 209−585) that lacks the 13 residues between amino acids 196 and 209. Removal of the sequence completely abolished the enzymatic activity of the catalytic core domain. No catalytic turnover was detected for Ubp15 (209−585) in hydrolyzing Ub-AMC even with an enzyme concentration as high as 200 nM. To test whether deletion of this stretch of sequence had an impact on the folding of the catalytic core domain, we conducted circular dichroism (CD) analysis of the catalytic domain with or without the linker sequence. As shown in Figure 3, the CD spectrum of Ubp15(209−585) is very similar to that of Ubp15(196−585). Using the software SOMCD that estimates the secondary

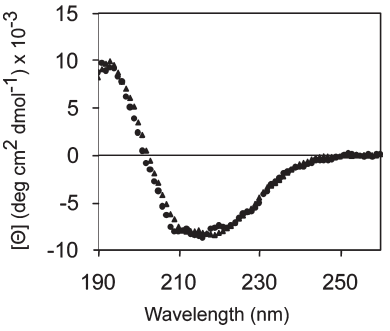

Figure 3. Circular dichroism spectra of the truncated Ubp15 containing the catalytic core domain. The far UV-CD spectra of Ubp15(196−585) (●) and Ubp15(209−585) (▲) are overlaid.

structure composition of a protein on the basis of UV circular dichroism data,[21] we showed that the secondary structure compositions of the two truncated Ubp15 core domains are almost identical (77% α-helix and 4% β-sheet as predicted). To further investigate the structural integrity of the Ubp15 core domains, we characterized the guanidine chloride (GdnHCl)-induced denaturation by circular dichroism. We found that Ubp15(209−585) and Ubp15(196−585) display similar denaturation profiles when being treated with different concentrations of GdnHCl (Figure S4 of the Supporting Information). Approximately 65% of the helical content was lost when the sample was treated with 5 M GdnHCl for both truncated proteins. Taken together, these results indicate that the deletion of the 13-amino acid sequence did not affect the overall folding of the catalytic core domain. On the basis of the modeled Ubp15 structure, the sequence corresponding to the 13-amino acid truncation is in the proximity of an active-site loop that contains the potential catalytic residue Asp482 and thus likely contributes to the organization of the active site into a productive conformation through direct contact.

Probing the Active Site by Site-Directed Mutagenesis. Multiple-sequence alignment of Ubp15 with several known USPs led to the identification of C214, H465, and D482 as potential catalytic residues (Figure S5 of the Supporting Information). Site-directed mutagenesis was used to confirm the identity of these active-site residues using the Ubp15(1−585) truncate. Each residue was individually mutated to alanine and purified as described in Materials and Methods. The steady-state rate constants were determined using Ub-AMC as a substrate. As expected, replacing the active-site Cys214 with alanine completely abolished the activity of Ubp15(1−585). No activity was detected with up to 400 nM enzyme. A more conservative mutant, C214S, was also found to be inactive under identical experimental conditions. Mutation of His465 to alanine resulted in a >70000-fold decrease in the k_{cat} value compared to that of wild-type Ubp15(1−585) [$k_{cat} = (0.10 \pm 0.01) \times 10^{-4}$ s^{-1}, and $K_m = 0.20 \pm 0.05$ μM]. Mutation of Asp482 to alanine led to insoluble protein.

Mutational Analysis of Ubiquitin-Binding Sites. Mutational analysis was used to identify ubiquitin-binding sites in Ubp15. We generated a model of Ubp15 bound with ubiquitin using the USP7−ubiquitin cocrystal structure as a template.[22] Specifically, the model was generated by the PHYRE protein fold recognition server[19] using the USP7 X-ray crystal structure as a template. Using Insight II (Accelrys, San Diego, CA), the modeled Ubp15 structure was superimposed on the cocrystal structure of USP7

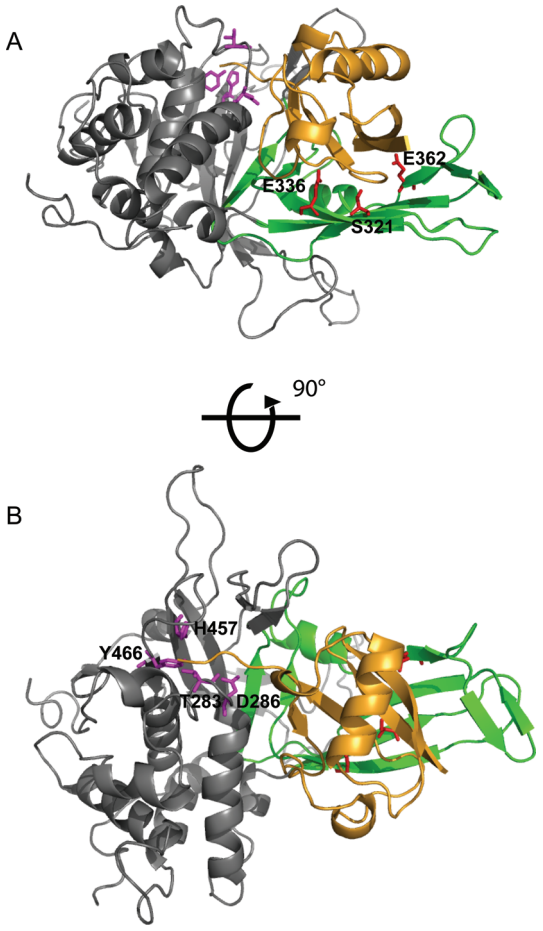

Figure 4. Model of the Ubp15 catalytic core (amino acids 196−554) in complex with ubiquitin. We generated a model of Ubp15 bound with ubiquitin using the USP7−ubiquitin cocrystal structure as a template.[22] Specifically, the model was generated by the PHYRE protein fold recognition server[19] using the USP7 X-ray crystal structure as a template. Using Insight II (Accelrys), the modeled Ubp15 structure was superimposed on the cocrystal structure of USP7 and ubiquitin aldehyde, which allowed the docking of ubiquitin to the Ubp15 model. Ubiquitin is colored orange. The finger subdomain of Ubp15 is colored green, while the rest of the catalytic core is colored gray. Ubp15 residues E336, E362, and S321 that form potential hydrogen bonds to the N-terminal face of ubiquitin are colored red (A), and residues D286, T283, H457, and Y466 that form potential hydrogen bonds to the C-terminal tail of ubiquitin are colored magenta (B). This image was generated using PyMol.

and ubiquitin aldehyde,[22] which allowed the docking of ubiquitin to the Ubp15 model. Extensive interactions were identified between the finger subdomain in the Ubp15 catalytic core and the ubiquitin surface close to the N-terminus (Figure 4A). Additional interactions exist between the C-terminal tail of ubiquitin and Ubp15 residues residing in or close to the active-site cleft (Figure 4B and Figure S6 of the Supporting Information). The contribution of Ubp15 residues to ubiquitin binding and catalysis was assessed by alanine scanning.

Mutation of Ser321, Glu362, and Glu336 that reside in the finger subdomain of the Ubp15 catalytic core individually to alanine led to a large decrease in catalytic efficiency (Table 2). E362A displayed a 62-fold increase in K_m compared to that of wild-type Ubp15. A 10-fold decrease in the k_{cat} value was also observed for the E362A mutant. E336A and S321A also exhibited large increases in K_m (22- and 7-fold, respectively), and substantial decreases in k_{cat} (24- and 18-fold, respectively).

Extensive interactions were also observed between the C-terminal tail of ubiquitin and the Ubp15 catalytic cleft in the modeled structure (Figure 4B and Figure S6 of the Supporting Information). Mutation of Ubp15 residues Thr283, Asp286, His457, and Tyr466, which are within hydrogen bonding distance of the ubiquitin C-terminal tail residues, to alanine led to substantial decreases in k_{cat} values. T283A exhibited a 14-fold decrease in k_{cat} compared to that of wild-type Ubp15. More dramatic effects were observed with the H457A, Y466A, and D286A mutants. The H457A and Y466A mutations led to 237- and 3.6×10^4-fold decreases in k_{cat}, respectively, while the D286A mutant was completely inactive. Interestingly, no significant changes in K_m were detected when T283, H457, and Y466 were mutated to alanine (Table 2).

Ubp15 Interacts with the Cell Cycle Activator Cdh1. A previous large-scale yeast interaction study has identified the WD40 repeat-containing protein, Cdh1, as a Ubp15-binding protein.[23] Recently, several WD40 repeat-containing proteins were found to stimulate DUB activity.[24−26] We were interested in determining whether Cdh1 regulates Ubp15's activity. We coexpressed Ubp15 and Cdh1 in Sf9 cells. Full-length Ubp15 was expressed with an N-terminal GST tag, while full-length Cdh1 was expressed with an N-terminal six-His tag. Using glutathione Sepharose resin, we were able to purify a protein complex containing GST-Ubp15 and His_6-Cdh1 from the co-infected insect cell lysate (Figure 5A). Conversely, we were also able to purify the Ubp15/Cdh1 complex using Ni-NTA affinity chromatography (Figure 5B). As a control, His_6-Cdh1 alone was transfected into Sf9 insect cells. The lysate was incubated with glutathione resin under identical experimental conditions. No Cdh1 was detected in any of the glutathione elution fractions (Figure 5C).

Western blotting was further used to corroborate the results of the SDS−PAGE analyses. The presence of Cdh1 was identified using a primary antibody specific for the N-terminal His tag in Cdh1. While Cdh1 was detected in glutathione elution fractions from cell lysate coexpressing full-length GST-Ubp15 and His_6-Cdh1, no Cdh1 was detected for cell lysate that lacked expression of full-length GST-Ubp15 (Figure 5D). Taken together, these observations confirmed that full-length Ubp15 physically interacts with Cdh1.

Cdh1 Does Not Stimulate Ubp15's Enzymatic Activity. Using Ub-AMC as a substrate, we determined the steady-state rate constants of the GST-Ubp15/His_6-Cdh1 sample purified using a nickel affinity column. In this sample, all Ubp15 exists in complex with Cdh1. We determined the concentration of Ubp15 on the basis of the relative band intensity of Ubp15 and Cdh1 on the SDS−PAGE gel measured using the Multiplex Band Analysis function of the FluorChem Q imaging system (Cell Biosciences). A k_{cat} value of $0.84 \pm 0.04\ s^{-1}$ was determined for the Ubp15/Cdh1 complex, close to the k_{cat} value determined for GST-Ubp15 alone ($1.23 \pm 0.02\ s^{-1}$). The K_m of 0.18 μM is also close to that determined for GST-Ubp15 alone (0.12 μM). No stimulation of Ubp15's activity by Cdh1 was observed. To further demonstrate that Cdh1 does not stimulate Ubp15's activity, we titrated Ubp15 with purified Cdh1, which has no DUB activity. No increase in Ubp15's activity was observed even with a 20-fold molar excess of Cdh1 added (Figure S7 of the Supporting Information). These results suggest that Cdh1 does not stimulate Ubp15's activity through formation of the complex. We also analyzed the potential effect of the GST tag on the kinetic

Table 2. Steady-State Kinetic Parameters of the Ubp15 Mutants

Ubp15 construct	k_{cat} (s^{-1})	K_m (μM)	k_{cat}/K_m (M^{-1} s^{-1})	x-fold decrease in k_{cat}	x-fold increase in K_m	x-fold decrease in k_{cat}/K_m
Ubp15(1−585)	0.71 ± 0.02	0.11 ± 0.01	6.5×10^6	1	1	1
E362A	0.072 ± 0.006	6.80 ± 0.75	1.1×10^4	10	62	591
E336A	0.030 ± 0.004	2.46 ± 0.59	1.2×10^4	24	22	542
S321A	0.040 ± 0.001	0.75 ± 0.05	5.3×10^4	18	7	123
T283A	0.052 ± 0.002	0.19 ± 0.02	2.7×10^5	14	1.7	24
D286A	no activity					
H457A	$(0.300 \pm 0.008) \times 10^{-2}$	0.09 ± 0.01	3.3×10^4	237	0.8	197
Y466A	$(0.20 \pm 0.02) \times 10^{-4}$	0.24 ± 0.08	83	3.6×10^4	2.2	7.8×10^4

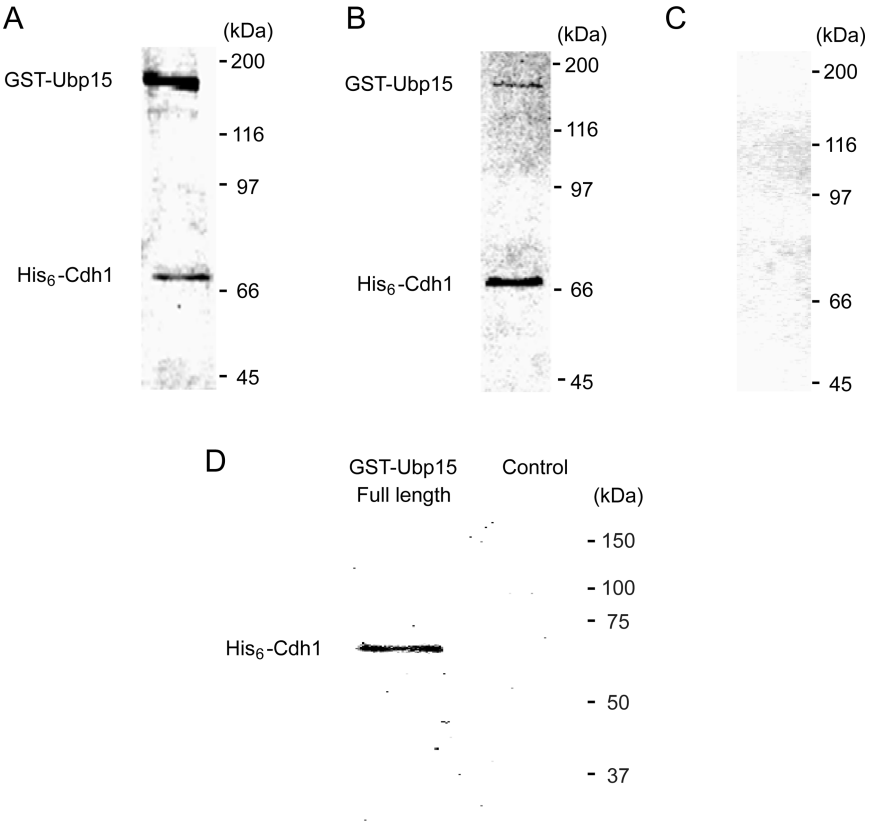

Figure 5. Purification of Ubp15 and Cdh1 as a complex. (A) Copurification of His_6-Cdh1 as a complex with full-length GST-Ubp15 using a glutathione affinity column from Sf9 cells expressing GST-Ubp15 and His_6-Cdh1. (B) Copurification of full-length GST-Ubp15 as a complex with His_6-Cdh1 using a nickel affinity column from Sf9 cells expressing GST-Ubp15 and His_6-Cdh1. (C) Insect cell lysate expressing His_6-Cdh1 was incubated with glutathione resin under the same experimental conditions described for panel A. No detectable amount of Cdh1 was identified in any of the glutathione elution fractions. Protein samples were separated via SDS−PAGE under reducing conditions and visualized by Coomassie Blue staining. (D) Western blot analysis of Cdh1 purified as a complex with full-length GST-Ubp15 using glutathione affinity resin. The presence of Cdh1 was detected using a primary antibody specific for the N-terminal six-His tag of Cdh1. As a control, insect cell lysate expressing only His_6-Cdh1 was incubated with glutathione resin, and no His_6-Cdh1 was detected in the eluted fraction. For all samples, approximately 1 μg of protein was loaded per lane.

parameters of full-length and truncated Ubp15 proteins (Table 1 and Figure S8 of the Supporting Information). When compared to the steady-state rate constants determined for His-tagged Ubp15 proteins, the k_{cat} or K_m values were not significantly altered by the GST tag.

The Ubp15 Terminal Domains Are Responsible for Formation of the Ubp15/Cdh1 Complex. To identify the domains in Ubp15 responsible for its interaction with Cdh1, several GST-Ubp15 truncations were coexpressed with full-length His_6-Cdh1. Both GST-Ubp15(1−585) and GST-Ubp15(196−1230) retained interaction with Cdh1 and copurified as a complex using a glutathione affinity column (Figure 6A,B). In contrast, the Ubp15 catalytic core domain (amino acids 196−585) was defective in forming a complex with Cdh1. SDS−PAGE analyses of eluted fractions from cells coexpressing GST-Ubp15(196−585) and full-length His_6-Cdh1 revealed no detectable bands of Cdh1 (Figure 6C). Furthermore, Western blot analyses identified significant amounts of copurified Cdh1 from insect cell lysate coexpressing GST-Ub15(1−585) or GST-Ubp15(196−1230) (Figure 6D). In contrast, only trace amounts of Cdh1 were identified in glutathione affinity-purified fractions when Cdh1 was coexpressed with GST-Ubp15(196−585) (Figure 6D). Our

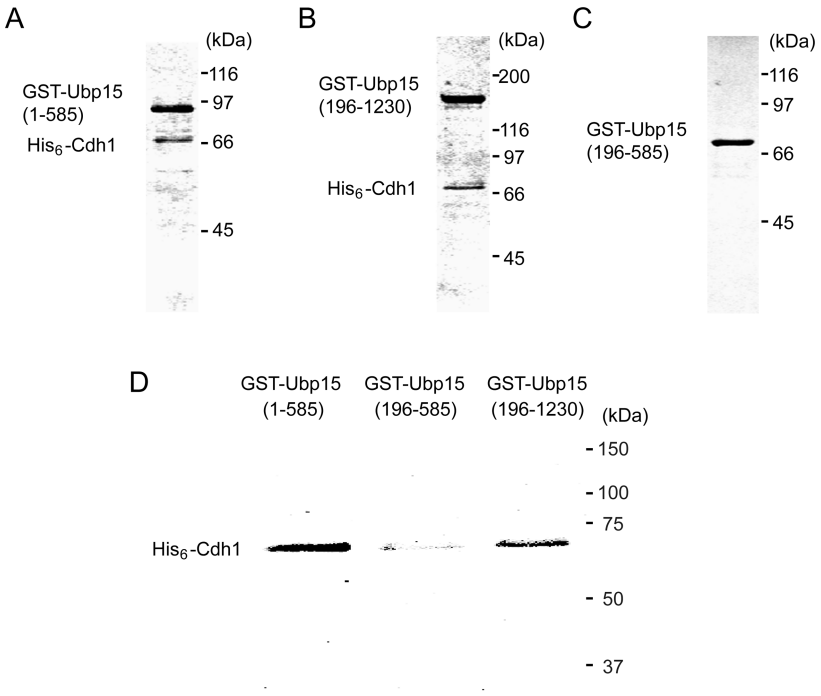

Figure 6. Requirement of the Ubp15 terminal domains for interaction with Cdh1. Various GST-Ubp15 truncates were coexpressed with His_6-Cdh1 in Sf9 insect cells and purified using a glutathione affinity column. Protein samples were separated via SDS−PAGE under reducing conditions and visualized by Coomassie Blue staining. Cdh1 was copurified as a complex with (A) GST-Ubp15(1−585) with a C-terminal domain truncation and (B) GST-Ubp15(196−1230) with a N-terminal domain truncation. (C) No Cdh1 was copurified with GST-Ubp15(196−585) that contains only the catalytic core domain. (D) Western blot analysis of formation of the Cdh1 complex with several GST-Ubp15 truncates. The presence of Cdh1 was detected using a primary antibody specific for the N-terminal six-His tag of Cdh1. For all samples, approximately 1 μg of protein was loaded per lane.

results indicate that the Ubp15 terminal domains are primarily responsible for its binding to Cdh1.

DISCUSSION

Many USPs exist as multidomain proteins, in which the catalytic core domain is usually flanked by N- and/or C-terminal domains. In this study, we showed that the terminal domains of Ubp15 regulate its deubiquitinating activity. While truncation of either terminal domain modestly reduced Ubp15's enzymatic activity, a more profound effect was observed when both terminal domains were removed. The Ubp15 catalytic core domain demonstrated a low level of activity despite the fact that it contains the essential catalytic elements and retains a normal fold. A similar observation was also made for human USP7, where the USP7 catalytic core demonstrated a >100-fold decrease in catalytic efficiency compared to that of full-length USP7.[15,16] A notable distinction is that the Ubp15 C-terminal domain deletion did not result in a decrease as pronounced as that observed in USP7. On the basis of a pairwise sequence alignment, we observed significant sequence similarity between Ubp15 and USP7, not just for the catalytic core domains (47% identical) but also for the N- and C-terminal domains (26 and 20% identical for the N- and C-terminal domains, respectively). Thus, a similar mechanism may be responsible for the stimulation of the catalytic activity of the catalytic core domain by the terminal domains in Ubp15 and USP7. A structural insight can be obtained from the high-resolution structure of the apo form of the USP7 catalytic domain and its complex with the mechanism-based inhibitor, ubiquitin aldehyde.[22] In the apo structure, the USP7 catalytic core contains a misaligned active site, in which the catalytic cysteine is approximately 9 Å from the triad histidine. Binding of ubiquitin aldehyde as a covalent adduct to the USP7 catalytic cysteine led to a productive conformation of the catalytic triad, in which the active-site cysteine moves to within 3.6 Å of the triad histidine. On the basis of this observation, it is possible that the catalytic triad in the isolated core domain may exist in a nonproductive conformation, which is reorganized into a productive conformation in the presence of the terminal domains. In particular, there may be interdomain protein interactions between the Ubp15's terminal domains and Ubp15's catalytic core that are responsible for locking the Ubp15 active site into an active conformation.

The presence of the complete linker sequence did not stimulate the activity of Ubp15's catalytic core to a level similar to that of the Ubp15 core domain with the N-terminal TRAF-like domain. This observation suggests that the essential role of the TRAF-like domain cannot be substituted by the linker sequence. Although little direct interaction between the catalytic core domain and the TRAF-like domain was observed in the Ubp15 model based on the USP7 X-ray crystal structure (Figure 2), in solution more interdomain interactions may exist and contribute to the stimulation of Ubp15 catalytic activity. Indeed, the equivalent linker sequence in USP7 has high temperature factors in crystals, suggesting a relatively flexible nature.[20] Further study using a solution technique such as small-angle X-ray scattering (SAXS) will likely provide further information about the mechanism of stimulation.

Interestingly, the C-terminal domain of Ubp15 stimulates the activity of the Ubp15 catalytic core domain to a level comparable to that observed for the N-terminal domain. Thus, the stimulatory effect of the N-terminal TRAF-like domain on Ubp15 activity can be largely compensated by the C-terminal domain. It is not clear whether the N- and C-terminal domains of Ubp15 modulate the activity of the catalytic domain through a similar mechanism. More structural and functional information about the C-terminal domain of Ubp15 will be needed to improve our understanding of the mechanism of stimulation.

Interestingly, Ubp15 has a K_m value (140 ± 10 nM) >100-fold lower than that of its homologue, USP7. This distinction may reflect on the varied affinity of the two DUBs for the ubiquitin moiety in the substrate. To probe ubiquitin binding by Ubp15, we generated a series of single-point mutations in the Ubp15 catalytic core domain that interact either with the N-terminal face or with the C-terminal tail of ubiquitin (Table 2). Besides the interaction between the C-terminal tail of ubiquitin and the Ubp15 active-site cleft, the N-terminal face of ubiquitin also interacts extensively with the finger subdomain of Ubp15 and contributes to ubiquitin binding and catalysis. Mutation of several conserved finger subdomain residues led to an elevated K_m value. In contrast, mutation of the Ubp15 active-site cleft residues that form potential hydrogen bonds with the C-terminal tail of ubiquitin had little impact on K_m despite a large decrease in k_{cat}. Our results indicate that ubiquitin binding in the Ubp15 exosite is essential for catalysis. The large increase in K_m values (22−62-fold) observed for two Ubp15 finger subdomain mutants (E336A and E362A) underlines the important contribution of Ubp15's finger subdomain to ubiquitin binding and catalysis. This may be common to other USP family DUBs because of the highly conserved catalytic core domain structure and the ubiquitin binding mode.

Interestingly, although mutations in the Ubp15 active-site cleft led to substantial decreases in the k_{cat} values for all the mutants tested, the K_m value seemed to be largely unaffected, which suggests that the interactions between the ubiquitin C-terminal tail residues and the Ubp15 active-site cleft contribute minimally to the binding of the ubiquitin moiety. Instead, the selected residues may mainly contribute to orient the ubiquitin C-terminal diglycine residues for efficient catalysis.

We confirmed that Cdh1 interacts with Ubp15 through copurification of Ubp15 and Cdh1 as a complex. Interestingly, both the N- and C-terminal domains of Ubp15 contribute to its interaction with Cdh1. The ability of DUBs to interact with proteins at multiple sites has recently been reported. It has been previously determined that the N-terminal TRAF-like domain of USP7 contains the mdm2/p53 binding site.[20] Another recent study further determined that the C-terminal domain of USP7 contains additional binding sites for both p53 and mdm2.[16] These studies together suggest that the USP terminal domains play important roles in binding cognate protein partners.

Recently, interactions between DUB and WD40 repeat-containing proteins have been reported. A recent global proteomic analysis in humans identified 774 interacting protein partners for 75 human DUBs.[27] Intriguingly, many of these proteins are WD40 repeat-containing proteins. Similarly, through large-scale proteomic analyses, eight of the 20 yeast Ubps were shown to physically interact with WD40 repeat-containing proteins.[23,28,29] Some of the DUB−WD40 repeat-containing protein interactions function to stimulate DUB activity, as in the human USP1/UAF1 complex.[24] In contrast, Cdh1 does not significantly stimulate Ubp15's activity (Figure S7 of the Supporting Information). Therefore, the stimulation of DUB activity in the USP family may occur in cis through interaction with domains in the same polypeptide as exemplified by the yeast Ubp15 and human USP7 or in trans through interaction with a separate interacting protein. On the basis of the stimulation of the DUB activity, the widespread USP−WD40 repeat-containing protein complexes can be divided into two groups, exemplified by Ubp15/Cdh1 and USP1/UAF1 complexes.

The cellular function of Ubp15 can be inferred from its interaction with Cdh1. Cdh1 functions to activate the APC/C complex, one of two major cell cycle E3 ubiquitin ligases, and also determines APC/C's substrate specificity. Although the Ubp15/Cdh1 interaction does not stimulate Ubp15's catalytic activity, the interaction may serve to recruit Ubp15 to the APC/C complex. Cdh1's interaction with Ubp15 may be dynamic in nature and form at only certain stages of the cell cycle. In accord with such a notion, the affinity between Ubp15 and Cdh1 is modest compared to that of the USP1/UAF1 complex that also contains a WD40 repeat-containing protein. The APC/C is responsible for targeting a number of cell cycle proteins to the proteasome during specific stages of the cell cycle. APC/C-mediated degradation of cell cycle proteins allows immediate changes in protein concentration and drives the transitions through the different stages of the cell cycle. An untimely ubiquitination or deubiquitination could lead to a faulty cell cycle progression causing apoptosis or genomic instability. The association of Ubp15 with the APC/C complex through Cdh1 represents an attractive mechanism in which Cdh1's WD40 repeat scaffold can reciprocally regulate the ubiquitin ligase and the DUB activities to achieve a tightly controlled ubiquitination of cell cycle proteins.

■ ASSOCIATED CONTENT

Supporting Information. Supporting figures (Figures S1−S8). This material is available free of charge via the Internet at http://pubs.acs.org.

■ AUTHOR INFORMATION

Corresponding Author

*Phone: (302) 831-8940. Fax: (302) 831-6335. E-mail: zzhuang@udel.edu.

■ ABBREVIATIONS

DUB, deubiquitinating enzyme; USP, ubiquitin-specific protease; Ubp, ubiquitin-specific processing protease; TRAF, TNF receptor-associated factor; Ub-AMC, ubiquitin-7-amino-4-methylcoumarin; UbVS, ubiquitin-vinyl sulfone; HAUSP, herpesvirus-associated ubiquitin-specific protease; CD, circular dichroism; GdnHCl, guanidine hydrochloride.

■ REFERENCES

(1) Chen, Z. J., and Sun, L. J. (2009) Nonproteolytic functions of ubiquitin in cell signaling. *Mol. Cell 33*, 275–286.

(2) Ulrich, H. D., and Walden, H. (2010) Ubiquitin signalling in DNA replication and repair. *Nat. Rev. Mol. Cell Biol. 11*, 479–489.

(3) Amerik, A. Y., Li, S. J., and Hochstrasser, M. (2000) Analysis of the deubiquitinating enzymes of the yeast *Saccharomyces cerevisiae*. *Biol. Chem. 381*, 981–992.

(4) Komander, D., Clague, M. J., and Urbe, S. (2009) Breaking the chains: Structure and function of the deubiquitinases. *Nat. Rev. Mol. Cell Biol. 10*, 550–563.

(5) Nijman, S. M., Luna-Vargas, M. P., Velds, A., Brummelkamp, T. R., Dirac, A. M., Sixma, T. K., and Bernards, R. (2005) A genomic and functional inventory of deubiquitinating enzymes. *Cell 123*, 773–786.

(6) Amerik, A. Y., and Hochstrasser, M. (2004) Mechanism and function of deubiquitinating enzymes. *Biochim. Biophys. Acta 1695*, 189–207.

(7) Reyes-Turcu, F. E., Ventii, K. H., and Wilkinson, K. D. (2009) Regulation and cellular roles of ubiquitin-specific deubiquitinating enzymes. *Annu. Rev. Biochem. 78*, 363–397.

(8) Hu, M., Li, P., Song, L., Jeffrey, P. D., Chenova, T. A., Wilkinson, K. D., Cohen, R. E., and Shi, Y. (2005) Structure and mechanisms of the proteasome-associated deubiquitinating enzyme USP14. *EMBO J. 24*, 3747–3756.

(9) Leggett, D. S., Hanna, J., Borodovsky, A., Crosas, B., Schmidt, M., Baker, R. T., Walz, T., Ploegh, H., and Finley, D. (2002) Multiple associated proteins regulate proteasome structure and function. *Mol. Cell 10*, 495–507.

(10) Samara, N. L., Datta, A. B., Berndsen, C. E., Zhang, X., Yao, T., Cohen, R. E., and Wolberger, C. (2010) Structural insights into the assembly and function of the SAGA deubiquitinating module. *Science 328*, 1025–1029.

(11) Kohler, A., Zimmerman, E., Schneider, M., Hurt, E., and Zheng, N. (2010) Structural basis for assembly and activation of the heterotetrameric SAGA histone H2B deubiquitinase module. *Cell 141*, 606–617.

(12) McCullough, J., Row, P. E., Lorenzo, O., Doherty, M., Beynon, R., Clague, M. J., and Urbe, S. (2006) Activation of the endosome-associated ubiquitin isopeptidase AMSH by STAM, a component of the multivesicular body-sorting machinery. *Curr. Biol. 16*, 160–165.

(13) Row, P. E., Liu, H., Hayes, S., Welchman, R., Charalabous, P., Hofmann, K., Clague, M. J., Sanderson, C. M., and Urbe, S. (2007) The MIT domain of UBPY constitutes a CHMP binding and endosomal localization signal required for efficient epidermal growth factor receptor degradation. *J. Biol. Chem. 282*, 30929–30937.

(14) Denuc, A., Bosch-Comas, A., Gonzalez-Duarte, R., and Marfany, G. (2009) The UBA-UIM domains of the USP25 regulate the enzyme ubiquitination state and modulate substrate recognition. *PLoS One 4*, e5571.

(15) Fernandez-Montalvan, A., Bouwmeester, T., Joberty, G., Mader, R., Mahnke, M., Pierrat, B., Schlaeppi, J. M., Worpenberg, S., and Gerhartz, B. (2007) Biochemical characterization of USP7 reveals post-translational modification sites and structural requirements for substrate processing and subcellular localization. *FEBS J. 274*, 4256–4270.

(16) Ma, J., Martin, J. D., Xue, Y., Lor, L. A., Kennedy-Wilson, K. M., Sinnamon, R. H., Ho, T. F., Zhang, G., Schwartz, B., Tummino, P. J., and Lai, Z. (2010) C-terminal region of USP7/HAUSP is critical for deubiquitination activity and contains a second mdm2/p53 binding site. *Arch. Biochem. Biophys. 503*, 207–212.

(17) Chen, Y. H., Yang, J. T., and Martinez, H. M. (1972) Determination of the secondary structures of proteins by circular dichroism and optical rotatory dispersion. *Biochemistry 11*, 4120–4131.

(18) Zapata, J. M., Martinez-Garcia, V., and Lefebvre, S. (2007) Phylogeny of the TRAF/MATH domain. *Adv. Exp. Med. Biol. 597*, 1–24.

(19) Kelley, L. A., and Sternberg, M. J. (2009) Protein structure prediction on the Web: A case study using the Phyre server. *Nat. Protoc. 4*, 363–371.

(20) Hu, M., Gu, L., Li, M., Jeffrey, P. D., Gu, W., and Shi, Y. (2006) Structural basis of competitive recognition of p53 and MDM2 by HAUSP/USP7: Implications for the regulation of the p53-MDM2 pathway. *PLoS Biol. 4*, e27.

(21) Unneberg, P., Merelo, J. J., Chacon, P., and Moran, F. (2001) SOMCD: Method for evaluating protein secondary structure from UV circular dichroism spectra. *Proteins 42*, 460–470.

(22) Hu, M., Li, P., Li, M., Li, W., Yao, T., Wu, J. W., Gu, W., Cohen, R. E., and Shi, Y. (2002) Crystal structure of a UBP-family deubiquitinating enzyme in isolation and in complex with ubiquitin aldehyde. *Cell 111*, 1041–1054.

(23) Ho, Y., Gruhler, A., Heilbut, A., Bader, G. D., Moore, L., Adams, S. L., Millar, A., Taylor, P., Bennett, K., Boutilier, K., Yang, L., Wolting, C., Donaldson, I., Schandorff, S., Shewnarane, J., Vo, M., Taggart, J., Goudreault, M., Muskat, B., Alfarano, C., Dewar, D., Lin, Z., Michalickova, K., Willems, A. R., Sassi, H., Nielsen, P. A., Rasmussen, K. J., Andersen, J. R., Johansen, L. E., Hansen, L. H., Jespersen, H., Podtelejnikov, A., Nielsen, E., Crawford, J., Poulsen, V., Sorensen, B. D., Matthiesen, J., Hendrickson, R. C., Gleeson, F., Pawson, T., Moran, M. F., Durocher, D., Mann, M., Hogue, C. W., Figeys, D., and Tyers, M. (2002) Systematic identification of protein complexes in *Saccharomyces cerevisiae* by mass spectrometry. *Nature 415*, 180–183.

(24) Cohn, M. A., Kowal, P., Yang, K., Haas, W., Huang, T. T., Gygi, S. P., and D'Andrea, A. D. (2007) A UAF1-containing multisubunit protein complex regulates the Fanconi anemia pathway. *Mol. Cell 28*, 786–797.

(25) Cohn, M. A., Kee, Y., Haas, W., Gygi, S. P., and D'Andrea, A. D. (2009) UAF1 is a subunit of multiple deubiquitinating enzyme complexes. *J. Biol. Chem. 284*, 5343–5351.

(26) Kee, Y., Yang, K., Cohn, M. A., Haas, W., Gygi, S. P., and D'Andrea, A. D. (2010) WDR20 regulates activity of the USP12 × UAF1 deubiquitinating enzyme complex. *J. Biol. Chem. 285*, 11252–11257.

(27) Sowa, M. E., Bennett, E. J., Gygi, S. P., and Harper, J. W. (2009) Defining the human deubiquitinating enzyme interaction landscape. *Cell 138*, 389–403.

(28) Gavin, A. C., Bosche, M., Krause, R., Grandi, P., Marzioch, M., Bauer, A., Schultz, J., Rick, J. M., Michon, A. M., Cruciat, C. M., Remor, M., Hofert, C., Schelder, M., Brajenovic, M., Ruffner, H., Merino, A., Klein, K., Hudak, M., Dickson, D., Rudi, T., Gnau, V., Bauch, A., Bastuck, S., Huhse, B., Leutwein, C., Heurtier, M. A., Copley, R. R., Edelmann, A., Querfurth, E., Rybin, V., Drewes, G., Raida, M., Bouwmeester, T., Bork, P., Seraphin, B., Kuster, B., Neubauer, G., and Superti-Furga, G. (2002) Functional organization of the yeast proteome by systematic analysis of protein complexes. *Nature 415*, 141–147.

(29) Krogan, N. J., Cagney, G., Yu, H., Zhong, G., Guo, X., Ignatchenko, A., Li, J., Pu, S., Datta, N., Tikuisis, A. P., Punna, T., Peregrin-Alvarez, J. M., Shales, M., Zhang, X., Davey, M., Robinson, M. D., Paccanaro, A., Bray, J. E., Sheung, A., Beattie, B., Richards, D. P., Canadien, V., Lalev, A., Mena, F., Wong, P., Starostine, A., Canete, M. M., Vlasblom, J., Wu, S., Orsi, C., Collins, S. R., Chandran, S., Haw, R., Rilstone, J. J., Gandi, K., Thompson, N. J., Musso, G., St. Onge, P., Ghanny, S., Lam, M. H., Butland, G., Altaf-Ul, A. M., Kanaya, S., Shilatifard, A., O'Shea, E., Weissman, J. S., Ingles, C. J., Hughes, T. R., Parkinson, J., Gerstein, M., Wodak, S. J., Emili, A., and Greenblatt, J. F. (2006) Global landscape of protein complexes in the yeast *Saccharomyces cerevisiae*. *Nature 440*, 637–643.